Temporal and spectral self-shifts of dark optical solitons

A. M. Weiner, R. N. Thurston, W. J. Tomlinson, J. P. Heritage, D. E. Leaird, and E. M. Kirschner

Bellcore, 331 Newman Springs Road, Red Bank, New Jersey 07701-7040

R. J. Hawkins

Lawrence Livermore National Laboratory, P.O. Box 808, Livermore, California 94550

Received February 2, 1989; accepted May 23, 1989

We report the discovery of temporal and spectral self-shifts of dark optical solitons propagating in single-mode fibers. These shifts become increasingly pronounced as the intensity and the fiber length are increased. We show that our data are in quantitative agreement with numerical solutions to a modified nonlinear Schrödinger equation that includes the Raman contribution to the nonlinear refractive index.

Bright and dark optical solitons in single-mode fibers are pulses for which the nonlinear refractive index exactly compensates the group-velocity dispersion (GVD), and thus the soliton pulses propagate without broadening.[1] Bright optical solitons, which occur in the negative GVD portion of the spectrum ($\lambda > 1.3$ μm in standard monomode fibers), have been investigated extensively over the past ten years.[2] Because of the difficulty of generating appropriate dark pulses, however, experimental tests of dark soliton propagation, predicted for positive GVD,[1] have been attempted only recently.[3–5] In Ref. 5 we reported the first, to our knowledge, unambiguous observation of the fundamental dark soliton. In this Letter we describe what is to our knowledge the first experimental study of high-power dark soliton propagation, and we report the discovery of temporal and spectral self-shifts of $\simeq$200-fsec dark solitons. Our data are in excellent agreement with numerical solutions to a modified nonlinear Schrödinger equation (NLSE), which includes an experimentally determined Raman response function[6] as part of the nonlinear refractive index.

Before undertaking our experiments, we performed extensive numerical simulations, based on the standard NLSE, of dark pulse propagation in fibers.[7] Dark solitons consist of a rapid dip in the intensity of a broad pulse or a cw background. The starting pulse for our calculations, and for our experiments as well, is a 185-fsec tangent hyperbolic dark pulse on a 1.76-psec Gaussian background pulse, i.e.,

$$E(t) = E_0 \tanh(t/T_1)\exp[-(t^2/T_2^2)],$$

where $T_1 = 0.1136$ psec and $T_2 = 1.388$ psec. This input pulse, an antisymmetric function of time with zero intensity and an abrupt π phase shift at its center, closely resembles the predicted analytical form of the fundamental dark (black) soliton.[1,5,7] The calculated intensity profiles of output pulses emerging from a 1.4-m length of fiber are shown in Fig. 1. In Fig. 1(a), which corresponds to low power and linear propagation, the output dark pulse is substantially broadened owing to GVD's acting alone. As the power is increased to the soliton power [Fig. 1(b)] the output dark pulse narrows, tending to the duration of the input, even though the background pulse, which is only $\simeq$10 times wider, spreads significantly.[7] At higher powers [Figs. 1(c) and 1(d)] the central black soliton narrows further and spawns a complementary pair of low-contrast (gray[5,7]) solitons, which separate symmetrically as the pulse travels down the fiber. The depth and the velocity of the gray solitons are increasing functions of input power.

Our experimental setup is described in detail elsewhere.[5] Briefly, 75-fsec, 0.62-μm pulses from a colliding-pulse mode-locked dye laser,[8] amplified at a 8.6-kHz rate by a copper-vapor-laser-pumped dye amplifier system,[9] are shaped by spatial masking within a temporally nondispersive lens and grating apparatus.[10] The resultant dark pulses were focused into a 1.4-m length of single-mode, polarization-preserving fiber. The temporal profiles of pulses emerging from the fiber were measured by cross correlation with unshaped 75-fsec pulses, and the spectra were measured by using a 0.32-m spectrometer and a photodiode ar-

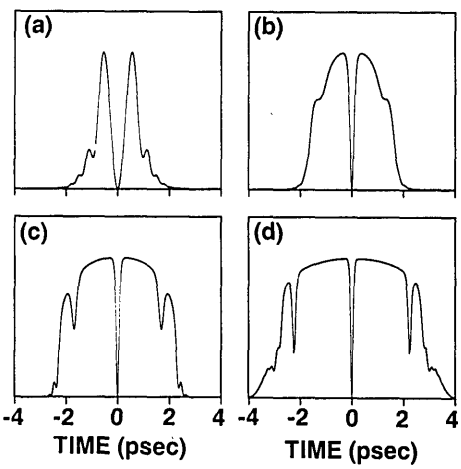

Fig. 1. Intensity profiles of output dark pulses from a 1.4-m fiber, calculated by using the standard NLSE. The peak input powers are (a) 1.5 W, (b) 150 W, (c) 450 W, and (d) 975 W.

0146-9592/89/160868-03$2.00/0

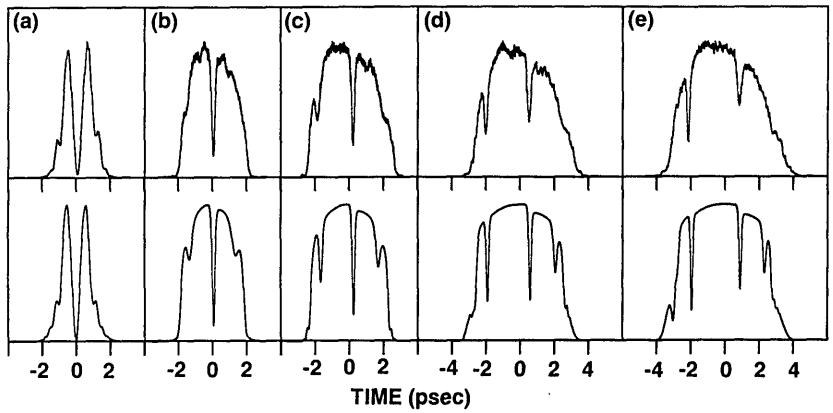

Fig. 2. Top traces: cross-correlation measurements of output dark pulses. Bottom traces: theoretical cross-correlation profiles, calculated by using a modified NLSE that includes the Raman contribution to the nonlinear index. The input peak powers are (a) 7.5 W, (b) 225 W, (c) 450 W, (d) 750 W, and (e) 975 W. The same horizontal scale is used for all the plots.

ray (spectral resolution $\simeq$0.17 nm). An attenuator wheel was used to control the input power to the fiber, and cross correlations and spectra were recorded as a function of input power.

Cross-correlation measurements of the output dark pulses are plotted in Fig. 2 (the upper traces) for peak input powers of 7.5 to 975 W. For powers below $\simeq$300 W, our data are in quantitative agreement with the predictions of the standard NLSE, and the fundamental dark soliton is clearly observed.[5] For powers above $\simeq$300 W, however, our data deviate significantly from the behavior suggested by Fig. 1. As the power is increased the central soliton progressively loses contrast, shifts to later times within the background pulse, and finally [Figs. 2(d) and 2(e)] broadens. Furthermore, only a single gray soliton, which appears near the rising edge of the background pulse and which grows narrower and deeper as the central soliton broadens and loses contrast, becomes evident. At the highest power examined (975 W) the gray soliton is considerably deeper than the remnant of the central black soliton, and its duration (175 fsec) is less than that of the input dark pulse.

We performed several tests to verify the significance and repeatability of our data. Experimentally, we performed measurements with 100-fsec dark pulses and with dark pulses on square (rather than Gaussian) backgrounds. In each case we obtained data similar to those shown in Fig. 2. Numerically, we ran simulations for starting pulses perturbed in a variety of ways; in no case could we duplicate the experimental trends. Thus the unpredicted features in our data—the shift, broadening, and loss of contrast of the central black soliton and the appearance of a single gray soliton instead of a gray soliton pair—signify a breakdown of the standard NLSE under our experimental conditions.

To augment the temporal data we measured the power spectra of the fiber output pulses (the upper traces in Fig. 3). At low power the spectrum exhibits two peaks symmetrically located about a central hole [Fig. 3(a)]. According to the standard NLSE, the spectrum should broaden symmetrically as the power is increased. Instead, the data show that for increasing power the spectra broaden preferentially toward the red, with the central hole shifting toward the blue. At the highest powers a second hole, corresponding to the pronounced gray soliton in the time-domain data,

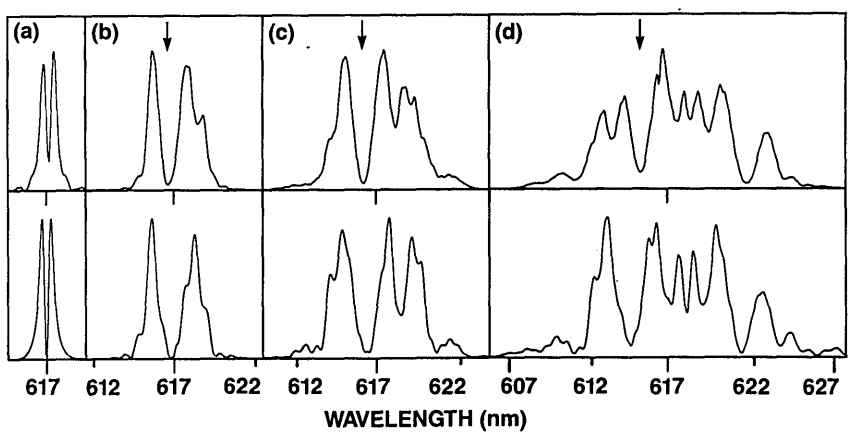

Fig. 3. Top traces: measured power spectra of output dark pulses. Bottom traces: theoretical power spectra, calculated by using the modified NLSE. The peak input powers are (a) 7.5 W, (b) 225 W, (c) 450 W, and (d) 975 W. In (b), (c), and (d) the arrow marks the location of the central hole, which shifts to the blue as the power is increased. The same horizontal scale is used for all the plots.

appears on the red side of the spectrum. The blue shift of the central hole and the excess spectral broadening toward the red suggest Raman amplification of longer-wavelength spectral components by the shorter-wavelength components. Analogous Raman self-pumping causes spectral red shifts[11,12] and fissioning[13,14] of subpicosecond-duration fundamental and higher-order bright solitons, respectively.

Computer solutions to a modified NLSE, which includes a time-dependent Raman response function as part of the nonlinear refractive index, accurately predict our data. Our time-domain formulation is fully equivalent to the usual approach in which Raman scattering is treated in the frequency domain. The treatment of the nonlinear polarization as a response function was introduced in Ref. 15; derivation of the Raman response function for silica-core fibers and a procedure for its inclusion in a modified NLSE are given in Ref. 6. Briefly, the response function is the Fourier transform of the Raman gain spectrum and comprises a series of rapidly damped oscillations, with an initial period of 75 fsec, corresponding to the inverse of the gain peak at 440 cm^{-1}.[6] Here we directly apply this Raman response function to model our dark pulse propagation experiments. Our calculations include no adjustable parameters.

Calculated temporal profiles and power spectra are plotted as the lower traces in Figs. 2 and 3, respectively. The calculated spectra quantitatively reproduce the blue shift of the central hole, the detailed shape of the spectra, and the position and strength of the second hole that appears at longer wavelengths. The computed temporal profiles, which have been convolved with a 75-fsec Gaussian to account for the cross correlations performed in the actual experiments, are in striking agreement with the data. Both the temporal shift of the central soliton and the enhancement of the negative-time gray soliton at the expense of its positive-time counterpart are clearly evident. Furthermore, the computations accurately predict the temporal positions of the various solitons in the data for all experimental power levels. Of course, some differences between experimental and numerical results do occur, especially at the highest powers. For example, the central soliton's loss of contrast is greater than that calculated, and its broadening is not predicted. For several reasons we believe that these discrepancies are caused by laser intensity fluctuations. Since at high powers the central dark pulse acquires a power-dependent velocity, intensity fluctuations translate into temporal jitter, which leads to the broadening and excess contrast loss observed in the measurements.

Self-shifts of dark optical solitons are in many ways analogous to those previously reported for bright solitons.[11–14] For example, spectral and temporal self-shifts of bright solitons are predicted to scale linearly and quadratically, respectively, with the fiber length.[12,13] Self-shifts of dark solitons are expected to scale in the same way. We investigated this point by repeating our cross-correlation measurements with a 4.1-m fiber; as expected, we observed temporal shifts considerably larger than those in Fig. 2. At $\simeq$300 W of input power, for example, the shift of the central soliton was $\simeq$500 fsec, compared with $\simeq$50 fsec for the 1.4-m fiber, in rough agreement with a quadratic length dependence. A second similarity relates to the relative strength of various perturbations to the NLSE. Numerical studies have shown that for 100-fsec bright solitons Raman self-pumping dominates third-order dispersion and self-steepening.[14] Likewise, we have performed simulations that demonstrate that these additional perturbations do not significantly affect dark pulse propagation under the current conditions. Of course there are also differences, most notably the fact that dark solitons, unlike bright solitons, do not form multiple-soliton bound states.[16]

In summary, we have investigated high-power propagation of $\simeq$200-fsec black solitons. Our study reveals a number of new phenomena that are not predicted by the standard NLSE, including temporal and spectral self-shifts of the central black soliton and creation of a single high-contrast gray soliton. Our data are in excellent agreement with numerical solutions to a modified NLSE that includes a Raman contribution to the nonlinear index.

The authors thank R. H. Stolen for helpful discussions. This research was performed in part under the auspices of the U.S. Department of Energy by Lawrence Livermore National Laboratory under contract W-7405-ENG-48.

References

1. A. Hasegawa and F. Tappert, Appl. Phys. Lett. **23,** 142, 171 (1973).
2. L. F. Mollenauer, R. H. Stolen, and J. P. Gordon, Phys. Rev. Lett. **45,** 1095 (1980); L. F. Mollenauer, R. H. Stolen, J. P. Gordon, and W. J. Tomlinson, Opt. Lett. **8,** 289 (1983).
3. P. Emplit, J. P. Hamaide, F. Reynaud, C. Froehly, and A. Barthelemy, Opt. Commun. **62,** 374 (1987).
4. D. Krokel, N. J. Halas, G. Giuliani, and D. Grischkowsky, Phys. Rev. Lett. **60,** 29 (1988).
5. A. M. Weiner, J. P. Heritage, R. J. Hawkins, R. N. Thurston, E. M. Kirschner, D. E. Leaird, and W. J. Tomlinson, Phys. Rev. Lett. **61,** 2445 (1988).
6. R. H. Stolen, J. P. Gordon, W. J. Tomlinson, and H. A. Haus, J. Opt. Soc. Am. B **6,** 1159 (1989).
7. W. J. Tomlinson, R. J. Hawkins, A. M. Weiner, J. P. Heritage, and R. N. Thurston, J. Opt. Soc. Am. B **6,** 329 (1989).
8. J. A. Valdmanis, R. L. Fork, and J. P. Gordon, Opt. Lett. **10,** 131 (1985).
9. W. H. Knox, M. C. Downer, R. L. Fork, and C. V. Shank, Opt. Lett. **9,** 552 (1984).
10. A. M. Weiner, J. P. Heritage, and J. A. Salehi, Opt. Lett. **13,** 300 (1988); A. M. Weiner, J. P. Heritage, and E. M. Kirschner, J. Opt. Soc. Am. B **5,** 1563 (1988).
11. F. M. Mitschke and L. F. Mollenauer, Opt. Lett. **11,** 659 (1986); E. M. Dianov, A. Ya. Karasik, P. V. Mamyshev, A. M. Prokhorov, V. N. Serkin, M. F. Stel'makh, and A. A. Fomichev, JETP Lett. **41,** 294 (1985).
12. J. P. Gordon, Opt. Lett. **11,** 662 (1986).
13. K. Tai and A. Hasegawa, Opt. Lett. **13,** 392 (1987).
14. W. Hodel and H. P. Weber, Opt. Lett. **12,** 924 (1987).
15. R. W. Hellwarth, A. Owyoung, and N. George, Phys. Rev. A **4,** 2342 (1971).
16. K. J. Blow and N. J. Doran, Phys. Lett. A **107,** 55 (1985).